10. T. L. Charlu, R. C. Newton, O. J. Kleppa, *Geochim. Cosmochim. Acta* **39**, 1487 (1975).
11. H. Takei, S. Hosoya, M. Ozima, in *Materials Science of the Earth's Interior*, I. Sunagawa, Ed. (Terra Scientific, Tokyo, 1984), pp. 107–130.
12. It is obviously impossible to obtain any statistical measure of uncertainty based on one experiment. However, this run appeared normal in all respects, and it is reasonable to assume an uncertainty similar to that obtained for the pyroxene. Obtaining enough perovskite for the five to eight replicate runs needed for meaningful statistics is at present far too time-consuming and costly.
13. Y. Fei, S. K. Saxena, A. Navrotsky, *J. Geophys. Res.* **95**, 6915 (1990).
14. A. Navrotsky in *High-Pressure Research in Mineral Physics*, M. Manghnani and Y. Syono, Eds. (Terra Scientific, Tokyo, 1987), p. 261; *Prog. Solid State Chem.* **17**, 53 (1987); in *Perovskite—A Structure of Great Interest to Geophysics and Materials Science*, A. Navrotsky and D. J. Weidner, Eds. (American Geophysical Union, Washington, DC, 1989), pp. 67–80.
15. $\Delta G(T,P)$ is the Gibbs free energy of reaction at an arbitrary pressure and temperature (equal to zero along the phase boundary); $\Delta G^0(T)$, $\Delta H^0(T)$, and $\Delta S^0(T)$ are the Gibbs free energy, enthalpy, and entropy of reaction at one atmosphere and the given temperature. $DV(P,T)$ is the volume change for the reaction at a given pressure and temperature; ΔV^0298 is the volume change at ambient conditions. C_p is heat capacity and ΔC_p is the difference in heat capacity of products and reactants.
16. D. J. Weidner, H. Sawamoto, H. Sasaki, M. Kumazawa, *J. Geophys. Res.* **89**, 7852 (1984).
17. D. J. Weidner and E. Ito, *Phys. Earth Planet. Inter.* **40**, 65 (1985).
18. A. Yeganeh-Haeri, D. J. Weidner, E. Ito, *Science* **243**, 787 (1989).
19. Y. Sumino and O. L. Anderson, in *CRC Handbook of Physical Properties of Rocks*, R. C. Carmichael, Ed. (CRC Press, Boca Raton, FL, 1984), vol. 3, pp. 39–138.
20. I. Suzuki, E. Ohtani, M. Kumazawa, *J. Phys. Earth* **27**, 53 (1979).
21. N. L. Ross and R. M. Hazen, *Phys. Chem. Minerals* **16**, 415 (1989).
22. E. Knittle, R. Jeanloz, G. L. Smith, *Nature* **319**, 214 (1986).
23. The data of Ross and Hazen (*21*) ($\alpha = 2.2 \times 10^{-5}$ K^{-1}) refer to temperatures between 75 and 300 K, whereas those of (*22*) ($\alpha = 4 \times 10^{-5}$ K^{-1}) refer to temperatures between 300 and 850 K. Although a higher thermal expansivity at higher temperatures is generally expected because of increasing anharmonicity, decomposition of perovskite to glass or pyroxene complicates the higher temperature data, and the value of α at temperatures greater than 500 K is uncertain. Pressure may be expected to decrease thermal expansivity by suppressing anharmonicity. Possible phase transitions in the perovskite at high pressures p and t temperatures (from orthorhombic to tetragonal to cubic) may also affect α. Thus the thermal expansivity under mantle conditions is not well-constrained, and we examine the effect of these uncertainties by doing two sets of calculations using different constant values of α.
24. Joint Committee on Powder Diffraction Standards, International Center for Diffraction Data, Swarthmore, PA (1988), cards 4-829 and 34-189.
25. I. Suzuki, *J. Phys. Earth* **27**, 53 (1979).
26. We thank M. Ozima for providing the orthopyroxene sample. Supported by U.S. National Science Foundation and Japan Society for the Promotion of Science.

8 May 1990; accepted 23 July 1990

Direct Measurement of Forces Between Linear Polysaccharides Xanthan and Schizophyllan

DONALD C. RAU AND V. ADRIAN PARSEGIAN

Direct osmotic stress measurements have been made of forces between helices of xanthan, an industrially important charged polysaccharide. Exponentially decaying hydration forces, much like those already measured between lipid bilayer membranes or DNA double helices, dominate the interactions at close separation. Interactions between uncharged schizophyllans also show the same kind of hydration force seen between xanthans. In addition to the practical possibilities for modifying solution and suspension properties through recognition and control of molecular forces, there is now finally the opportunity for theorists to relate macroscopic properties of a polymer solution to the microscopic properties that underlie them.

POLYSACCHARIDES HAVE A CAPACITY to stabilize cellular or colloidal suspensions, an ability to maintain or even to facilitate bulk transport in muci and gels, and a high interaction specificity in cell recognition; they are used industrially to the extent of the millions of metric tons. The key to understanding these properties seems to be in understanding the physical interactions of these molecules with each other as well as with their aqueous environment. We now report direct measurements by the osmotic stress method (*1, 2*) of hydration forces between molecules of uncharged schizophyllan and of charged xanthan, both stiff linear polysaccharides.

These measurements offer an opportunity to relate directly measured molecular interactions to macroscopic solution properties. For example, we may now undertake an entirely new kind of investigation to relate the molecular basis of the hydrodynamic radius with the strength of perturbation of boundary water. Further, we can now expect to relate changes in forces with changes in solution viscosity, hygroscopic power, and gel-forming properties. This power might, in turn, lead to systematic design of better stabilizers of practical importance and provide the opportunity to relate directly measured interactions to the chemical identity of surfaces.

The most remarkable feature of this interaction occurs at surface separations of 2 to 10 Å where there is an exponentially varying force with a decay length of ~3.3 Å, totally unlike expectations from electrostatics, van der Waals interactions, or molcular packing entropies. This is very much like the "hydration force" seen, again by osmotic stress measurements, between electrically neutral or charged phospholipid bilayers (*3*) and between DNA double helices (*4, 5*) at comparable separations in many different ionic solutions. The observation of dominating hydration forces between these polysaccharides suggests an important role for these interactions in determining their function and properties.

Measured forces between xanthans show little dependence on the kind or concentration of salt. From a practical viewpoint, there is a remarkable correlation between the properties of this material seen by our measurements and the qualities that make it so valuable in food technology, oil recovery, and other industrial applications. The same molecular stiffness that imparts high solution viscosity causes mutual alignment at well-defined separation; the same hygroscopic power that stabilizes suspensions under all ionic conditions is seen as a hydration force insensitive to the kind and concentration of salt in the suspending medium.

Osmotic stress has been used in quantitative force measurement for at least 15 years, beginning with forces between phospholipid bilayer membranes (*1, 2*). Recently it has been developed to reveal both force and motion of DNA molecules as well as of membranes in thermodynamically well-defined assemblies (*5, 6*). This method is based on the ability of an "indifferent polymer" [for example, polyethylene glycol (PEG) or polyvinylpyrolidone (PVP) or dextran], to phase separate from many biopolymers, particularly stiff, hydrophilic macromolecules in aqueous solution. The osmotic pressure of the polymer in its phase exerts a force on the macromolecular phase that is balanced at equilibrium by the intermolecular repulsion between the biopolymers. Small ions and water are free to move between the two phases. Distances between macromolecules, equilibrated against a known PEG or PVP solution osmotic pressure and salt environment, are determined from the spacing of the interaxial reflections observed by x-ray

Laboratory of Biochemistry and Metabolism, National Institute of Diabetes and Digestive and Kidney Diseases, and Physical Sciences Laboratory, Division of Computer Research and Technology, Building 12A, Room 2007, National Institutes of Health, Bethesda, MD 20892.

scattering (7). The end result is an intermolecular force curve as interaxial spacings are measured over a range of PEG or PVP osmotic pressures (8). These spacings are equilibrium thermodynamic measurements, independent of cycling between high and low pressures and temperatures.

The structure and physical properties of xanthan have been extensively investigated (9). The repeating chemical structure of xanthan is shown below.

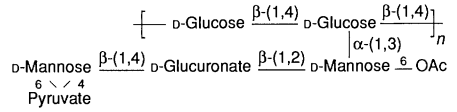

A trisaccharide arm is covalently linked to alternate glucoses of a cellulose backbone. In addition to the charged carboxylate group of the side chain glucuronate sugar, acid-labile, ketal-linked pyruvate groups are found on approximately one-half of the terminal mannoses of our xanthan. Electron microscopy (10) suggests that both stiff single- and double-stranded helices exist as ordered forms. The fiber diffraction pattern has been fitted for both single- and double-stranded forms (11). Both structures are a fivefold helix of the repeating pentasaccharide unit shown above. The diameter is ~21 Å.

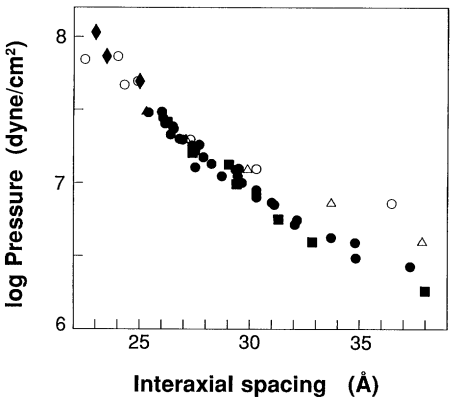

Fig. 1. Forces between parallel xanthan molecules in NaCl solutions. ○, 0.1 M NaCl, 10 mM tris-Cl (pH 7.5), and 1 mM EDTA; NaCl was varied as follows: △, 0.2 M; ●, 0.4 M; ■, 0.8 M; and ◆, 1.0 M. Forces are plotted as the osmotic stress on a hexagonal lattice of molecular rods versus interaxial separation. Note similarity of forces at interaxial distances was less than 33 Å. In all preparations, lyophilized xanthan (23) was dissolved in 10 mM tris-Cl (pH 7.5) and 1 mM EDTA (10-1 TE) to a concentration of about 2 mg/ml. The solution was clarified by centrifugation (20,000*g*, 1 hour, and 4°C); the clear supernatant (about 1 mg/ml) was extensively dialyzed against 10-1 TE and used without further purification. Consistent, x-ray quality ordering of xanthan under a variety of ionic conditions and osmotic pressures was achieved by initially forming a precipitate either by gently layering 0.3 ml of xanthan (1 mg/ml) in 10-1 TE on 1 ml of 25% PEG (20,000 average molecular weight) in 0.5 M NaCl and 10-1 TE, or by layering 1 ml of ethanol on 0.3 ml of xanthan (1 mg/ml) in 0.5 M sodium acetate and 10-1 TE. Well-formed pellets can be centrifuged further after 24 hours at room temperature. The supernatant is drawn off and replaced by PEG-salt solutions of known osmotic pressure and ionic conditions. The bathing PEG-salt solution for the pellet was changed several times during several weeks.

The dependence of the osmotic pressure, Π, of a lattice of xanthan molecules on interaxial spacing and NaCl concentration, over the range 0.1 to 0.8 M, is shown in Fig. 1. Especially in the range of separations 23 to 33 Å, all data sets overlap almost completely. At greater separations there is indication of a stronger repulsion between molecules in solutions of lower salt concentration.

Even stronger consistency is evident in xanthan-xanthan repulsion in solutions of 0.4 M NaCl and of four $MgCl_2$ concentrations (5 to 100 mM) (Fig. 2). In all cases the force decay is mainly exponential,

$$\Pi = A \exp(-D_{int}/\lambda)$$

with a decay distance, λ, of ~3.3 Å and a coefficient, A, of 7.3×10^{10} erg/cm^3 that is insensitive to salt concentration. Univalent Na^+, as compared with divalent Mg^{2+}, makes little difference in the strength of the observed force.

Force curves show a slight but distinct sideways break between two regions at about log(Π) = 7.1 with essentially equal exponential decay rates. This abrupt shift in the repulsive curve might be due either to a small change in xanthan conformation that reduces intermolecular forces or, in the absence of good higher order reflections, to a change in helical packing.

The effect of other counterions on the force was compared with Na^+ and Mg^{2+} (Fig. 3). Forces again seem robust when 50 mM $MgCl_2$ is replaced by 50 mM $CaCl_2$. The force in Ca^{2+} solution is at most only 20 to 30% weaker than in Mg^{2+}. But repulsion is noticeably weaker in solution of 10 mM trivalent cobalt hexammine $[Co(NH_3)_6Cl_3]$ by about a factor of 2 at a 25 Å separation. The apparent exponential decay length is also distinctly shorter than for the other counterions, 2.5 versus 3.3 Å.

Xanthan offers the opportunity to relate the chemical composition of the surface and physical properties (12, 13). Forces between chemically modified xanthans are shown in Fig. 4. Removal of acetyl groups from the 6′ hydroxyls of the side chain proximal mannoses has no noticeable effect on forces between xanthans. The removal of pyruvate groups, however, causes a clear decrease in repulsive force magnitude at 0.2 M NaCl. At low pressures, the force magnitude decreases by 30 to 40%, with no apparent change in the decay length. At higher pressures, the abrupt decrease in spacing is more pronounced than for unmodified xanthan but occurs at about the same pressure. The hydration force magnitude is about three times smaller than for unmodified xanthan at 25 Å separation, but decay lengths are only slightly different, 2.9 versus 3.3 Å.

The repeating chemical unit of of schizophyllan is shown below.

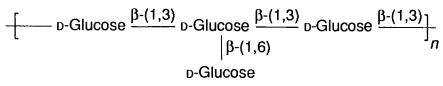

Composed solely of glucose monomers, the polymer adopts a triple helical conformation in aqueous solution (14). The most notable physical difference from xanthan is that schizophyllan is entirely uncharged. At high concentrations, a cholesteric liquid crystalline phase is formed (15). A proposed model for the triple-stranded helix (16) is a twofold helix of the tetrasaccharide unit with an 18 Å repeat spacing. The helix diameter is not well defined. A hydrated diameter of ~25 Å best fits the hydrodynamic data (17). A diameter of ~17 Å is estimated from the partial specific volume and mass per unit length (18). The diameter of the cylinder that just circumscribes the triple helix is most probably between these two estimates.

Repulsion between these uncharged triple helices (Fig. 5) is strikingly similar to that between the xanthans (also shown in this figure for comparison). Measured with three different stressing polymers [PEG-8 and PEG-20 (PEG of average molecular weights of 8,000 and 20,000, respectively) and PVP] at 5° and 20°C, there is a smooth-

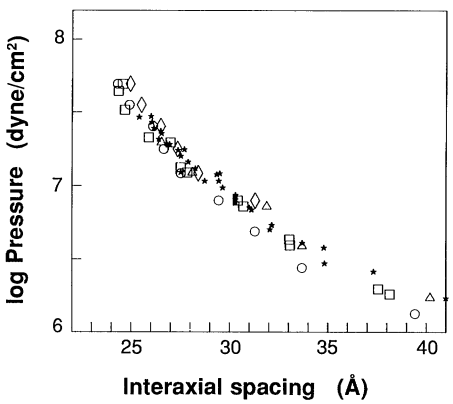

Fig. 2. Forces between xanthans in $MgCl_2$ solutions. ◇, 5 mM $MgCl_2$ and 10 mM tris-Cl (pH 7.5); $MgCl_2$ was varied as follows: △, 20 mM; □, 50 mM; and ○, 100 mM. ★, 0.4 M NaCl, 10 mM tris-Cl (pH 7.5), and 1 mM EDTA. Note the close similarity of forces at all separations.

ly varying force that might be interpreted as two different kinds of interaction below and above interaxial spacings of ~22 Å. If the diameter of the schizophyllan triple helix is ~20 Å, then the very rapidly increasing force observed at spacings less than 22 Å could well be due to steric collision between interpenetrating helical neighbors. At larger separations, however, the force appears exponential, with decay length of ~3.4 Å and coefficient 7.2×10^9 erg/cm^3. Temperature and the identity of the stressing polymer make no observable difference in measured forces.

Schizophyllan is not maintained in its own phase at pressures less than about log(Π) = 6.0 with either PEG or PVP, precluding force measurement at larger separations.

Thus, including our previous DNA results (*4, 5*), we now have direct intermolecular force measurements for three stiff helical biopolymers. The most remarkable feature of these force curves is that at close approach the same class of repulsion is observed. Independent of ionic strength and counterion species, independent of surface charge density (xanthan and DNA) or of whether the biopolymer is charged or not (schizophyllan), we observe an approximately exponentially increasing force with an apparent decay length of 3.0 to 3.5 Å for surface separations of 10 to 15 Å or less. These force characteristics compelled us to conclude for DNA, as for neutral lipid bilayers in distilled water, that this repulsion is due to the structuring of water between biopolymers. The data in no way look like the power law dependence expected for steric repulsion between hard, flexible rods (*5*). With these additional measurements, hydration forces (*19*) seem very probably a general and dominating feature of the interactions between all water-soluble surfaces at close approach. No other force appears to have comparable strength.

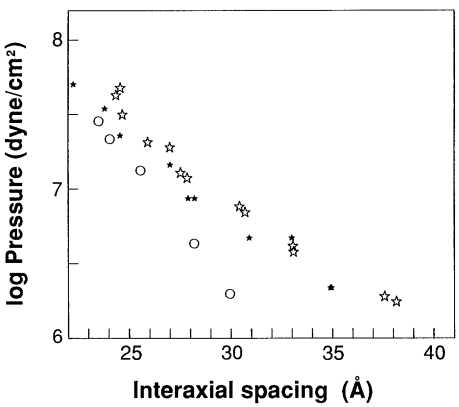

Fig. 3. Comparison of inter-xanthan forces in other counterions. ☆, 50 mM $MgCl_2$ and 10 mM tris-Cl (pH 7.5); ★, 50 mM $CaCl_2$ and 10 mM tris-Cl (pH 7.5); ○, 10 mM $Co(NH_3)_6Cl_3$ and 10 mM tris-Cl (pH 7.5).

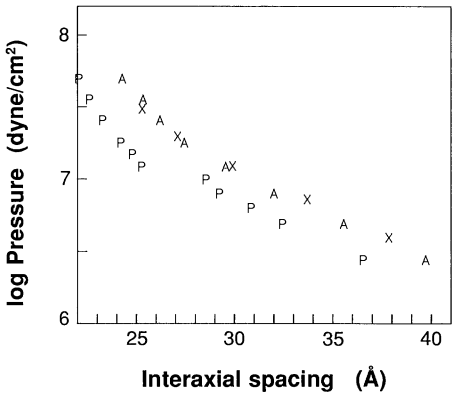

Fig. 4. Effect of acetate and pyruvate removal on xanthan forces measured in solutions of 0.2 M NaCl, 10 mM tris-Cl (pH 7.5), and 1 mM EDTA. X, unmodified xanthan; P, xanthan − pyruvate groups; and A, xanthan − acetyl groups. Xanthan samples with the pyruvate groups removed from terminal side-chain mannoses and with acetyl groups removed from proximal mannoses were prepared as described in (*12*) and exhaustively dialyzed against 10-1 TE.

From a theoretical viewpoint, it is the insensitivity of the several force curves to system variables such as ionic species and concentration that is most remarkable. Even though highly charged, xanthans repel with an exponentially decaying force that seems to vary weakly if at all with the ionic strength of the bathing medium. The exponential decay rate, 3.3 Å, is within experimental error of that observed previously between DNA double-helical polyelectrolytes in NaCl solutions whose repulsion at surface separations less than about 10 to 15 Å is dominated by surface hydration (*4, 5*). Force magnitudes between DNA molecules, though, clearly depend on the kind of ion in solution. The net hydration of the surface reflects not only the hydration of the DNA surface itself but also the hydration of ions bound to it, similar to the "secondary hydration" of mica surfaces with variously bound ions (*20*). In contrast, force magnitudes between xanthans are not observably different when we compare NaCl and $MgCl_2$ solutions and are only slightly decreased in $CaCl_2$ solution. Only forces in trivalent cobalt hexammine solution are appreciably different, with a reduced magnitude and a somewhat faster decay rate.

The insensitivity of forces to ion type suggests that there is either little or no ion binding or no secondary hydration due to bound ions, which could be buried within the helix. The exceptional action of trivalent cobalt hexammine (Fig. 3), which appreciably reduces the observed force and its decay rate, is due probably to binding to the negatively charged surface carboxylates. In identical cobalt hexammine solutions, however, DNA will bind sufficient trivalent ions to precipitate spontaneously from solution (*21*). The force curves of Co^{3+}-assembled helices have been interpreted as showing that attractive hydration forces are responsible for precipitation (*22*). The faster decay length observed for xanthan in cobalt hexammine could be due to trivalent binding insufficient for spontaneous assembly but sufficient to shorten the decay length.

Although forces at close approach appear dominated by water structuring and not by electrostatic double-layer interactions between charged surfaces, the power of charged surface groups to organize water is clearly apparent in the force curves. Forces between charged xanthans as compared with those between uncharged schizophyllan helices are an order of magnitude stronger at a 25 Å separation. The removal of neutral acetyl groups from xanthan side chains, exposing neutral hydryoxyls, has no observable effect on forces. In contrast, the remov-

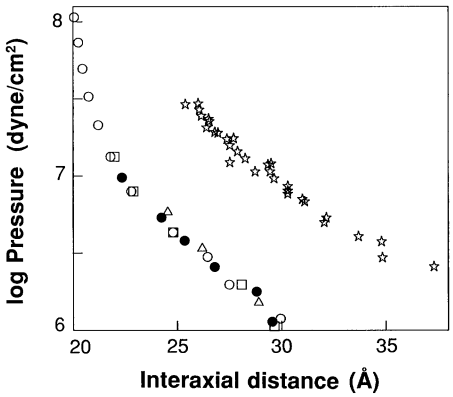

Fig. 5. Forces between schizophyllan helices in 1 mM tris (pH 7.5), at 5°C (●, with PEG at molecular weight 8,000) and 20°C (open symbols), with different stressing agents. ○, PEG of average molecular weight 8,000; □, PEG at 20,000; and △, PVP of average molecular weight 40,000. Forces between xanthan helices in 0.4 M NaCl are also shown (☆) for comparison. Schizophyllan (*24*) was dissolved in 0.1 mM EDTA (pH 7) to a final concentration of 1 mg/ml. Small aggregates were removed by centrifugation (20,000*g*, 1 hour, and 4°C), and the clear supernatant was dialyzed against 0.1 mM EDTA. The solution was then concentrated to about 20 mg/ml using a Centricon micro-concentrator with a cutoff filter for a molecular weight of 10,000 (Amicon Corp.) and used in the osmotic stress experiments without further purification. Initial pellets of schizophyllan with sufficient order for x-ray measurement were prepared either by layering 15 μl of the concentrated schizophyllan (20 mg/ml) on about 0.3 ml of 40% PEG (20,000 average molecular weight) or by layering about 30 μl of ethanol on 15 μl of schizophyllan (20 mg/ml). Precipitates are formed overnight at room temperature and pelleted by centrifugation. The supernatant was replaced by PEG or PVP salt solutions and equilibrated several weeks with at least three changes of the bathing solution.

al of charged pyruvate groups (accounting for about one-third of the total xanthan charge), exposing neutral hydroxyls, reduces the magnitude of the high-pressure, hydration force magnitude by about a factor of 3.

Biologically, the groups that modify sugars in long-chain polysaccharides include phosphates, sulfates, carboxylates, and amino groups. Each group has its own hydration and ion-binding characteristics that modulate interactions with other molecules. Through extensive measurements of many carbohydrates, specific contributions of different groups on hydration interactions can be compiled in much the same way as assigning charge to groups for electrostatic interaction. Cells use a wide range of carbohydrate structures to accomplish a wide range of functions. The only way to establish a structure-function relation is to understand first the structure-interaction relation.

REFERENCES AND NOTES

1. D. M. LeNeveu, R. P. Rand, V. A. Parsegian, *Nature* **259**, 601 (1976); ———, D. Gingell, *Biophys. J.* **18**, 209 (1977); R. P. Rand, *Annu. Rev. Biophys. Bioeng.* **10**, 277 (1981).
2. V. A. Parsegian, R. P. Rand, N. L. Fuller, D. C. Rau, *Methods Enzymol.* **127**, 400 (1986).
3. R. P. Rand and V. A. Parsegian, *Biochim. Biophys. Acta* **988**, 351 (1989).
4. D. C. Rau, B. K. Lee, V. A. Parsegian, *Proc. Natl. Acad. Sci. U.S.A.* **81**, 2621 (1984); V. A. Parsegian, R. P. Rand, D. C. Rau, in *Physics of Complex and Supermolecular Fluids*, S. A. Safran and N. A. Clark, Eds. (Wiley, New York, 1987), pp. 115–135.
5. R. Podgornik, D. C. Rau, V. A. Parsegian, *Macromolecules* **22**, 1780 (1989); R. Podgornik and V. A. Parsegian, *ibid.* **23**, 2265 (1990).
6. C. R. Safinya *et al.*, *Phys. Rev. Lett.* **57**, 2718 (1986).
7. An Enraf Nonius fixed-anode Diffractis 601 x-ray generator equipped with a high-power, fine-focus copper tube was used for the measurement of interaxial distances. The cameras were designed and built for our particular requirements [C. P. Mudd, H. Tipton, V. A. Parsegian, D. C. Rau, *Rev. Sci. Instrum.* **58**, 2110 (1987)]. The sample cells contain both the pellet and 100 μl of the bathing PEG (or PVP) and salt solution. X-ray reflections from the polysaccharide pellets are detected by film (DEF 5, Eastman-Kodak Co.). The strong interaxial reflections can be measured either by hand or by scanning densitometer (*5*). The 14.5 Å Bragg reflection from powdered *p*-bromobenzoic acid was used to calibrate the sample to film distance (about 15 cm). The intensities of the higher order reflections that determine the interhelical packing geometry were not strong enough to confirm unambiguously an expected hexagonal packing of rods for either xanthan or schizophyllan. We nonetheless assume that the packing is hexagonal and that the interhelical spacing, D_{int} is given by $D_{int} = 2D_{Br}/\sqrt{3}$, where D_{Br} is the Bragg spacing of the x-ray reflection.
8. Polyethylene glycol, average molecular weights 8,000 and 20,000, and polyvinylpyrrolidone, average molecular weight 40,000, were purchased from Sigma and used without further purification. A tabulation of osmotic pressures for PEG and PVP solutions is given in (*2*). We use the PVP osmotic pressures determined by us from secondary osmometry against PEG rather than the pressures given by K. A. Granath [*J. Colloid Sci.* **13**, 308 (1958)].
9. For a review of xanthan structure, properties and industrial uses, see D. A. Rees, E. R. Morris, D. Thom, J. K. Madden, in *The Polysaccharides*, G. O. Aspinall, Ed. (Academic, New York, 1982), vol. 1, pp. 195–290; P. A. Sandford and J. Baird, in *The Polysaccharides*, G. O. Aspinall, Ed. (Academic, New York, 1983), vol. 2, pp. 411–490.
10. G. Holzwarth and E. B. Prestridge, *Science* **197**, 757 (1977); B. T. Stokke, A. Elgsaeter, O. Smidsrod, *Int. J. Biol. Macromol.* **8**, 217 (1986).
11. R. Moorhouse, M. D. Walkinshaw, S. Arnott, *ACS (Am. Chem. Soc.) Symp. Ser.* **45**, 90 (1977); K. Okuyama *et al.*, *ibid.* **141**, 411 (1980).
12. T. Coviello, K. Kajiwara, W. Burchard, M. Dentini, *Macromolecules* **19**, 2826 (1986).
13. K. P. Shatwell, I. W. Sutherland, S. B. Ross-Murphy, *Int. J. Biol. Macromol.* **12**, 71 (1990).
14. T. Norisuye, T. Yanaki, H. Fugita, *J. Polym. Sci. Polym. Phys. Ed.* **18**, 547 (1980); T. Sato, T. Norisuye, H. Fujita, *Macromolecules* **16**, 185 (1983).
15. T. Itou and A. Teramoto, *Macromolecules* **17**, 1419 (1984); T. Odijk, *ibid.* **19**, 2313 (1986).
16. ———, T. Matsuo, H. Suga, *Carbohydr. Res.* **160**, 243 (1987).
17. T. Yanaki, T. Norisuye, H. Fujita, *Macromolecules* **13**, 1462 (1980); T. Kashiwagi, T. Norisuye, H. Fujita, *ibid.* **14**, 1220 (1981).
18. H. Enomoto, Y. Einaga, A. Teramoto, *ibid.* **18**, 2695 (1985).
19. For an overview, see "Proceedings on Hydration Forces and Molecular Aspects of Solvation," in *Chem. Scr.* **25**, 1–120 (1985).
20. R. M. Pashley, *Adv. Colloid Interface Sci.* **16**, 57 (1982).
21. J. Widom and R. L. Baldwin, *J. Mol. Biol.* **144**, 431 (1980).
22. D. C. Rau and V. A. Parsegian, in preparation.
23. Highly purified, high molecular weight xanthan was a gift from I. Heilweil.
24. Schizophyllan was a gift from A. Teramoto (Osaka University). The viscosity-determined average molecular weight of this fractionated sample is about 2×10^5 (A. Teramoto, personal communication).
25. The xanthan measurements were originally suggested to us by W. Schowalter, R. Prud'homme, and I. Heilweil. We thank I. Heilweil, G. Holzwarth, S. B. Ross-Murphy, and F. H. Kirkpatrick for several helpful textual suggestions.

19 December 1989; accepted 19 June 1990

Fragments of the HIV-1 Tat Protein Specifically Bind TAR RNA

KEVIN M. WEEKS, CHRISTOPHE AMPE, STEVE C. SCHULTZ, THOMAS A. STEITZ, DONALD M. CROTHERS

Proteolytically produced carboxyl-terminal fragments of the human immunodeficiency virus type–1 (HIV-1) Tat protein that include a conserved region rich in arginine and lysine bind specifically to transactivation response RNA sequences (TAR). A chemically synthesized 14-residue peptide spanning the basic subdomain also recognizes TAR, identifying this subdomain as central for RNA interaction. TAR RNA forms a stable hairpin that includes a six-residue loop, a trinucleotide pyrimidine bulge, and extensive duplex structure. Competition and interference experiments show that the Tat-derived fragments bind to double-stranded RNA and interact specifically at the pyrimidine bulge and adjacent duplex of TAR.

TAT IS A POTENT TRANSACTIVATOR OF HIV-1 long terminal repeat (LTR)–linked gene expression and is essential for viral replication (*1*). The transactivator is a small protein that includes a cysteine-rich region, which may be involved in zinc-mediated dimerization (*2*), a putative activation domain (*3, 4*), and a highly basic region (Fig. 1A). The precise mechanism of Tat-mediated transactivation remains unresolved (*5, 6*) but requires TAR, which is located at the 5′ end of the untranslated leader region of all viral messenger RNAs (mRNAs), the first 57 nucleotides of which form a stable stem-loop structure in vitro (*7*) (Fig. 1E). Nucleotides spanning positions +19 to +42 are sufficient for Tat response in vivo (*8, 9*). TAR must be located immediately downstream of the transcriptional start site; inversion of the sequence such that the complementary strand is transcribed eliminates transactivation (*7, 10*). Mutations that disrupt base pairing in duplex regions adjacent to the loop in TAR interfere with transactivation; compensating mutations that restore base pairing restore Tat responsiveness (*11, 12*). Point mutations in the loop eliminate Tat response (*11*), and Tat-mediated transactivation is also lost when sequences flanking the minimal TAR element are mutated such that competing secondary structures are more stable than the native TAR hairpin (*13*). Thus both RNA structure and primary sequence affect transactivation.

One hypothesis consistent with the accumulated data is that a direct interaction between Tat and TAR mediates transactivation. The formation of a specific complex between Tat purified from *Escherichia coli*

K. M. Weeks, Department of Chemistry, Yale University, New Haven, CT.
C. Ampe, Department of Molecular Biophysics and Biochemistry, Yale University, New Haven, CT.
S. C. Schultz, Department of Molecular Biophysics and Biochemistry and Howard Hughes Medical Institute, Yale University, New Haven, CT.
T. A. Steitz, Department of Molecular Biophysics and Biochemistry, Department of Chemistry, and Howard Hughes Medical Institute, Yale University, New Haven, CT.
D. M. Crothers, Department of Chemistry and Department of Molecular Biophysics and Biochemistry, Yale University, New Haven, CT.